ELSEVIER

Journal of Alloys and Compounds 293–295 (1999) 140–145

Journal of ALLOYS AND COMPOUNDS

Microstructures and defect structures in intermetallic compounds in the La–Ni alloy system

H. Inui*, T. Yamamoto, Zhang Di[1], M. Yamaguchi

Department of Materials Science and Engineering, Kyoto University, Sakyo-ku, Kyoto 606-8501, Japan

Abstract

Microstructures and defect structures in intermetallic compounds in the La–Ni alloy system have been investigated by transmission electron microscopy in the composition range of La–77.8~83.2 at.%Ni, which corresponds to compositions between two intermetallic phases, La_2Ni_7 and $LaNi_5$. The intermetallic phase, La_5Ni_{19} of the Ce_5Co_{19}-type is found for the first time to exist as an equilibrium phase at a composition between La_2Ni_7 and $LaNi_5$. This phase is stable at high temperatures around 1000°C but decomposes into La_2Ni_7 and $LaNi_5$ below 900°C. Numerous stacking faults are observed on basal planes in La_5Ni_{19} but the density of these basal stacking faults is greatly reduced in La_2Ni_7. Most stacking faults in La_5Ni_{19} are identified to be of the inter-block layer type while most of those in La_2Ni_7 are identified to be of the intra-block-layer type.

Keywords: $LaNi_5$; Stacking fault; Polytype; Transmission electron microscopy

1. Introduction

Alloys based on the intermetallic phase, $LaNi_5$ have been used as negative electrode materials of rechargeable nickel–metal hydride (Ni–MH) batteries because of their fast activation, high storage-capacity, long cycle-life and excellent electrochemical charge/discharge kinetics [1–4]. The phase diagram of the La–Ni binary system has repeatedly been the subject of investigation [5–8] and the recent version of the diagram [9] indicates that eight intermetallic phases, La_3Ni, La_7Ni_3, LaNi, La_2Ni_3, La_7Ni_{16}, $LaNi_3$, La_2Ni_7 and $LaNi_5$, exist in the equilibrium state and that no stable intermetallic phase has been reported to exist between La_2Ni_7 and $LaNi_5$. $LaNi_5$ has the $CaCu_5$-type hexagonal structure with $a=0.5017$ nm and $c=0.3987$ nm. The unit cell of a series of compounds in the La–Ni system, $LaNi_3$ and La_2Ni_7 is made of some block layers, each consisting of one unit layer of the $LaNi_2$ (Laves)-type and some unit layers of the $LaNi_5$-type [10]. The number of $LaNi_5$-type unit layers in a block layer (n) is 1 and 2 for $LaNi_3$ and La_2Ni_7, respectively. Thus, this series of compounds are formulated to be LaNix with $x=(5n+4)/(n+2)$ [10]. Depending on the stacking sequence of block layers along the c-axis, several modifications called polytypes are expected to occur for these compounds. For example, the hexagonal and rhombohedral modifications are formed for the double (AB) and triple (ABC) stacking of block layers, respectively. According to the Ramsdel notation [11], these are termed 2H and 3R modifications, respectively. Although no relevant experimental observations are available, such modifications with compositions between La_2Ni_7 and $LaNi_5$ are also possible by changing numbers of $LaNi_5$ and $LaNi_2$ unit layers consisting of each of the block layers stacked along the c-axis.

Thus, we decided to investigate microstructures and defect structures in intermetallic compounds in the La–Ni system as a function of alloy composition in the range of La–77.8~83.2 at.%Ni, which corresponds to compositions between La_2Ni_7 and $LaNi_5$.

2. Experimental procedures

Alloys with five different compositions of Ni/La (in atomic percent)=3.5, 3.8, 4.0, 4.5 and 5.0 were prepared by Ar-arc melting of high-purity (4N-grade) La and Ni. For the sake of simplicity, alloy compositions are ex-

*Corresponding author. Tel.: +81-75-753-5467; fax: +81-75-753-5461.

E-mail address: inui@karma.mtl.kyoto-u.ac.jp (H. Inui)

[1]Present address: State Key Laboratory of Metal Matrix Composites, Shanghai Jiao Tong University, Shanghai 200030, People's Republic of China.

0925-8388/99/$ – see front matter
PII: S0925-8388(99)00314-X

pressed as $LaNi_x$ with x being the Ni/La ratio throughout this paper. After arc-melting, all alloys were annealed at 930°C for 48 h in vacuum, and then furnace-cooled. Some of $LaNi_{3.8}$ alloys were annealed at 900 and 1000°C for 168 h in vacuum, and then water-quenched. Microstructures of these alloys were examined by scanning electron microscopy (SEM) and transmission electron microscopy (TEM). Thin foils for TEM observations were perforated by a standard double-jet thinning method at a voltage of 10 V with a solution of perchloric acid and methanol (2:8 by volume) kept at −40°C.

3. Results and discussion

3.1. Microstructures of La–Ni alloys

Microstructures of $LaNi_{5.0}$, $LaNi_{4.5}$, $LaNi_{4.0}$ and $LaNi_{3.5}$ alloys annealed at 930°C are shown in Fig. 1(a)–(d), respectively. These SEM images were taken in a back-scattered-electron imaging mode where phases with higher Ni contents are imaged darker. The $LaNi_{5.0}$ alloy exhibits a single-phase microstructure consisting of the $LaNi_5$ phase (Fig. 1(a)). The $LaNi_{3.5}$ alloy also exhibits essentially a single-phase microstructure consisting of the La_2Ni_7 phase (the region C), although some other phases are sporadically observed (for example, regions E and D in Fig. 1(d)). The brightness of these regions in the image together with the results of EDS (energy-dispersive spectroscopy) analyses imply that the regions D and E correspond to $LaNi_3$ and La_7Ni_{16} phases, respectively. The $LaNi_{4.0}$ alloy exhibits a three-phase microstructure (Fig. 1(c)). In addition to $LaNi_5$ (region A) and La_2Ni_7 (region C) phases, there is a phase (region B) with a composition in between these two phases. This phase is also observed in the $LaNi_{4.5}$ alloy (Fig. 1(b)), forming a two-phase microstructure with the $LaNi_5$ phase.

Fig. 2(a)–(c) shows TEM microstructures of $LaNi_{5.0}$, $LaNi_{4.5}$ and $LaNi_{3.5}$ alloys annealed at 930°C, respectively. Electron diffraction and EDS analyses have confirmed that $LaNi_{5.0}$ and $LaNi_{3.5}$ alloys are essentially of single phase, consisting respectively of $LaNi_5$ and La_2Ni_7 phases, whereas the $LaNi_{4.5}$ alloy (Fig. 2(b)) is of two-phase, consisting of the $LaNi_5$ phase (the lower half of the figure) and the phase with a composition between the $LaNi_5$ and La_2Ni_7 phases (the upper half of the figure). The La_2Ni_7 phase contains a small number of stacking faults on basal planes (Fig. 2(c)). On the other hand, the $LaNi_5$ phase is virtually featureless (Fig. 2(a)) except for sporadically observed dislocations. This is also the case for the $LaNi_5$ phase in the $LaNi_{4.5}$ alloy (Fig. 2(b)). The phase with a composition between $LaNi_5$ and La_2Ni_7 phases always contains numerous stacking faults, as seen in Fig. 2(b).

Selected-area electron diffraction (SAED) patterns taken along $\langle 11\bar{2}0\rangle$ and $\langle \bar{1}100\rangle$ directions of the $LaNi_5$ phase are depicted in Fig. 3(a) and (b), respectively. The SAED

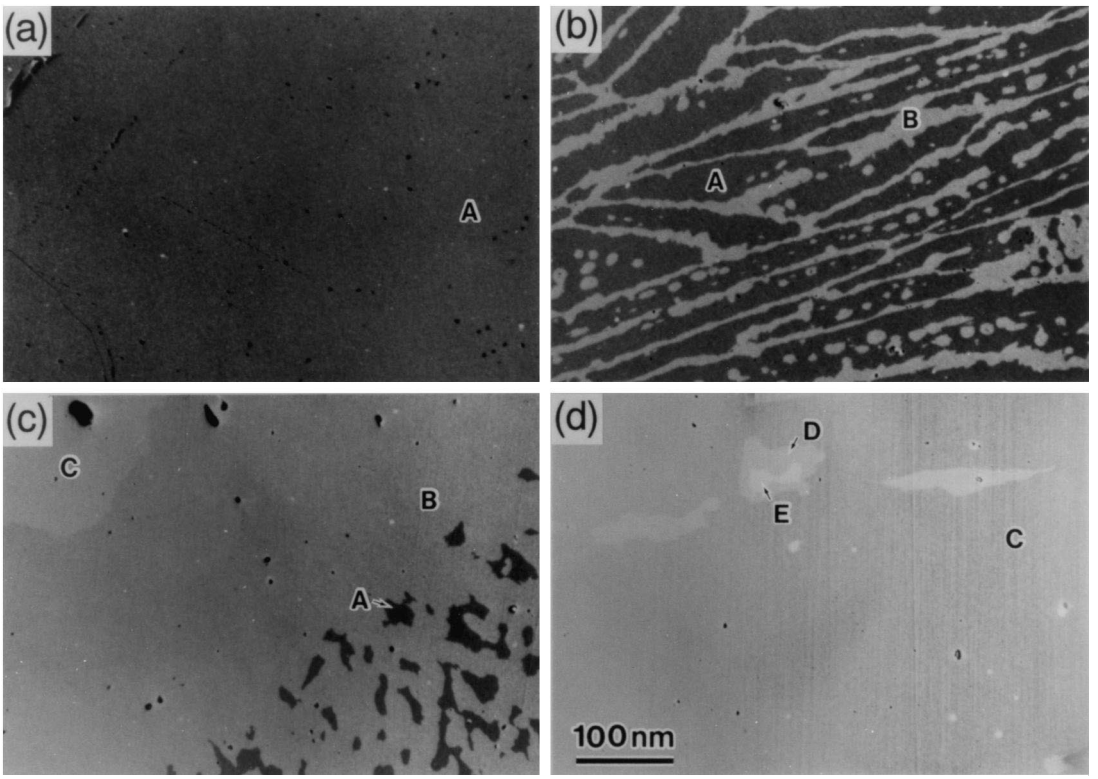

Fig. 1. SEM microstructures of La–Ni alloys annealed at 930°C for 48 h; (a) $LaNi_{5.0}$, (b) $LaNi_{4.5}$, (c) $LaNi_{4.0}$ and (d) $LaNi_{3.5}$ alloys.

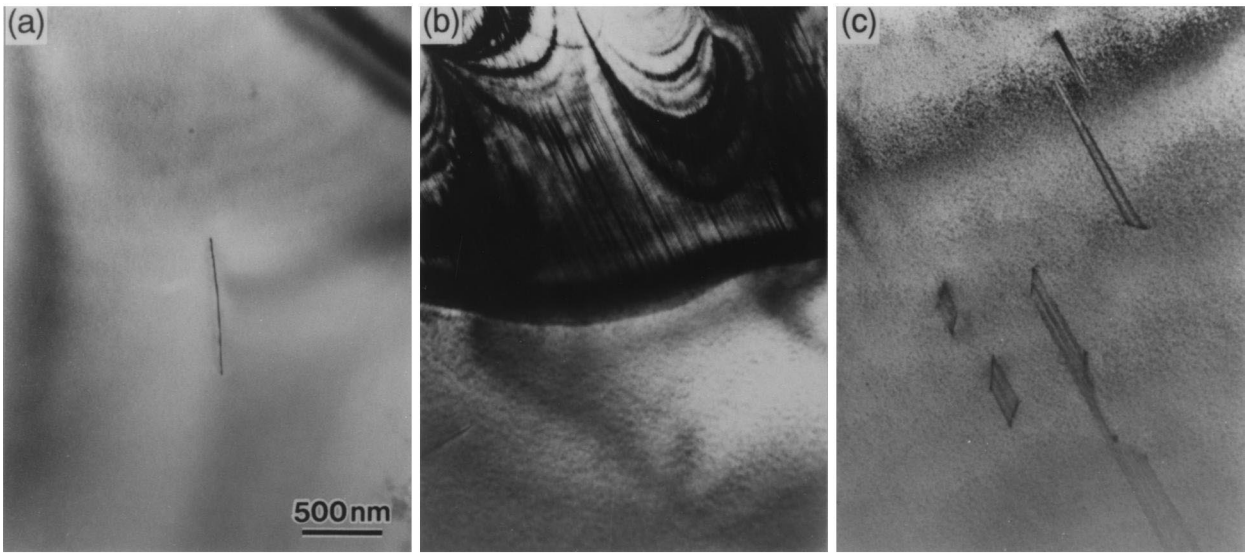

Fig. 2. TEM microstructures of La–Ni alloys annealed at 930°C for 48 h; (a) $LaNi_{5.0}$, (b) $LaNi_{4.5}$ and (c) $LaNi_{3.5}$ alloys.

patterns taken along the corresponding directions for the phase with a composition between the $LaNi_5$ and La_2Ni_7 phases and the La_2Ni_7 phase are presented in Fig. 3(c) and (d) and Fig. 3(e) and (f), respectively. The SAED patterns from the La_2Ni_7 phase (Fig. 3(e) and (f)) are consistently indexed assuming the phase to be a polytype of the Ce_2Ni_7 (2H)-type. We did not observe any evidence for the occurrence of the other polytype of the Gd_2Co_7 (3R)-type for the La_2Ni_7 phase. The SAED patterns from the phase with a composition between the $LaNi_5$ and La_2Ni_7 phases (Fig. 3(c) and (d)) are consistently indexed as those from the La_5Ni_{19} phase of the Ce_5Co_{19} (3R)-type, in which the unit cell is composed of three block layers stacked along the *c*-axis with each block layer consisting of one unit layer of the $LaNi_2$ (Laves)-type and three unit layers of the $LaNi_5$-type. Although the occurrence of the Ce_5Co_{19}-type phase has been reported in many binary systems consisting of rare-earth and transition-metals [9], this is the first

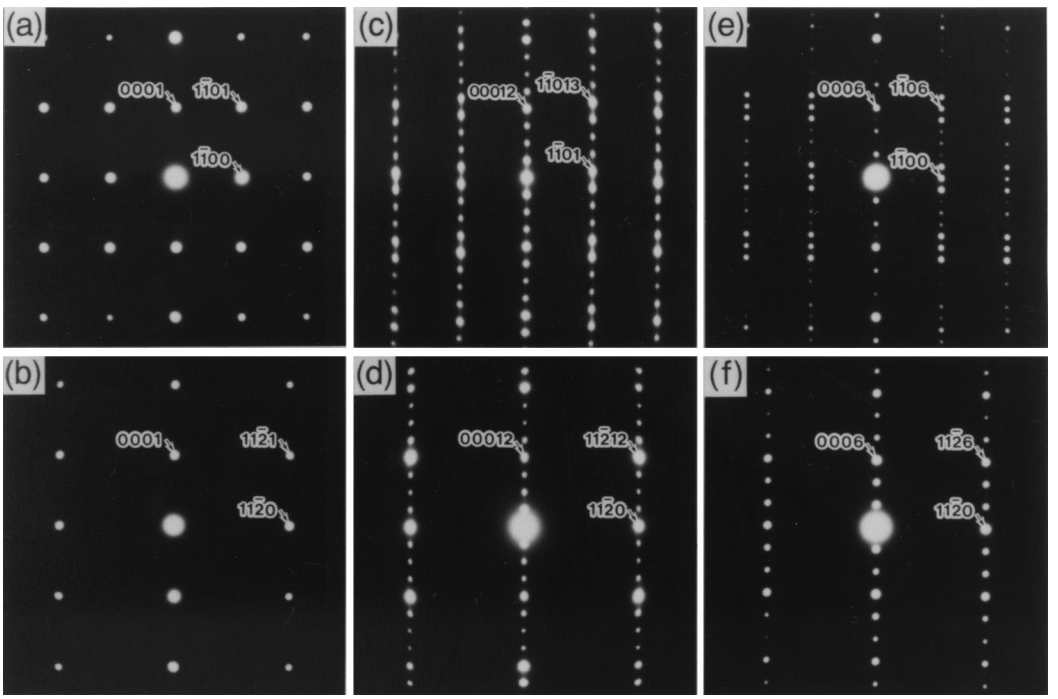

Fig. 3. Selected-area electron diffraction patterns taken along $\langle 11\bar{2}0\rangle$ and $\langle \bar{1}100\rangle$ directions of $LaNi_5$ (a,b), La_5Ni_{19} (c,d) and La_2Ni_7 (e,f) phases.

report on the occurrence of the phase in the La–Ni binary system. The La_5Ni_{19} phase is found to be stable only above 1000°C, since the $LaNi_{3.8}$ alloy exhibits essentially a La_5Ni_{19} single-phase microstructure when quenched from 1000°C whereas when quenched from 900°C, it exhibits a $LaNi_5 + La_2Ni_7$ two-phase microstructure.

3.2. Defect structures in intermetallic compounds in the La–Ni system

A typical example of high-resolution TEM images of the La_5Ni_{19} phase quenched from 1000°C is shown in Fig. 4(a) with the viewing direction parallel to [11$\bar{2}$0]. Examination

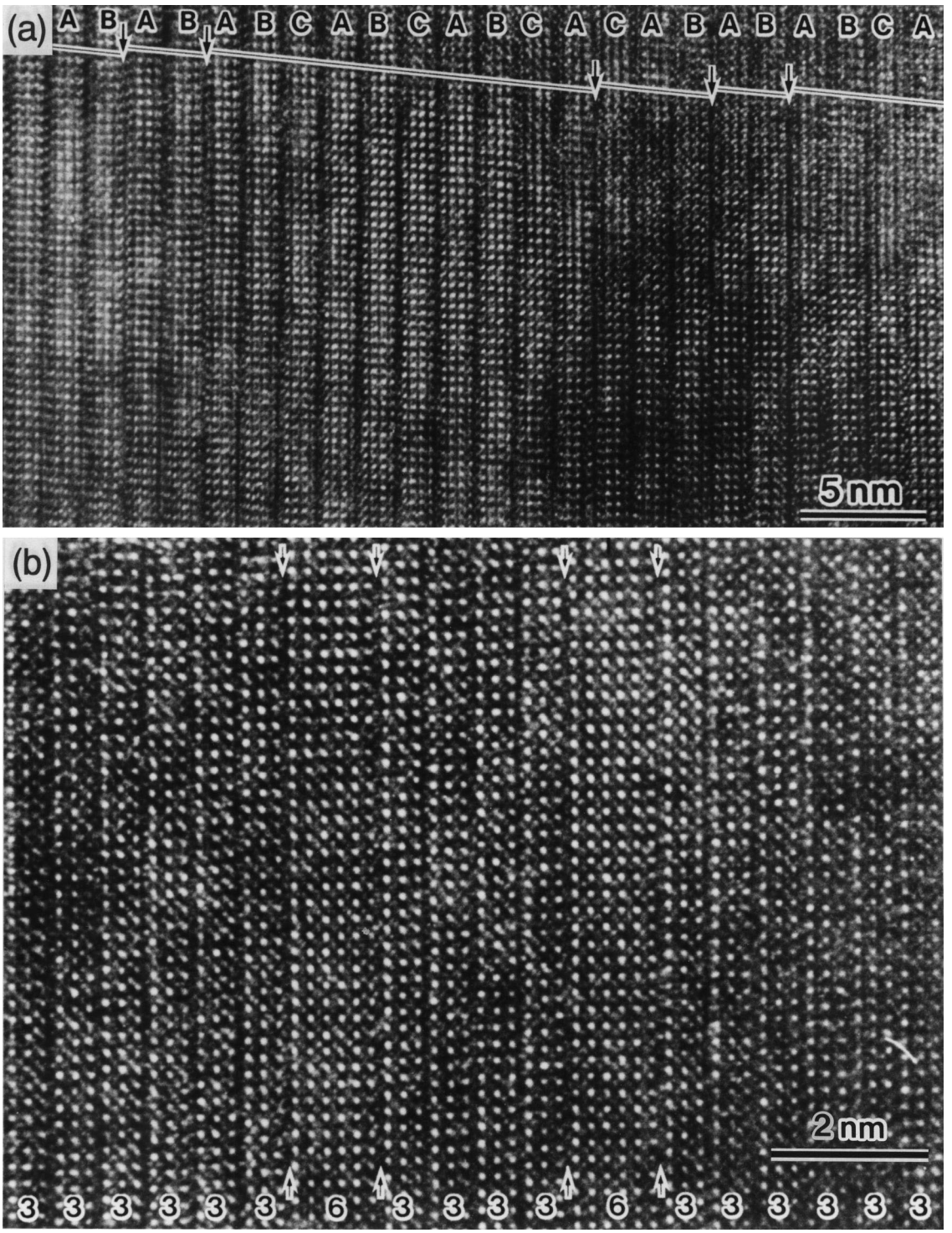

Fig. 4. High-resolution TEM image of stacking faults in (a) La_5Ni_{19} and in (b) La_2Ni_7 viewed along [11$\bar{2}$0].

of stacking positions of block layers has confirmed that the La_5Ni_{19} phase is based on the 3R modification with the ABC-type stacking sequence of block layers and revealed that most of stacking faults on basal planes are of the inter-block-layer type, in which faulting in the stacking sequence of block layers occurs, keeping the number of unit layers in block layers constant (one unit layer of the $LaNi_2$ (Laves)-type and three unit layers of the $LaNi_5$-type), as their positions are indicated by arrows. Such faulting mostly occurs as if one block layer is removed to form a stacking fault of the intrinsic type. As a result, the two-layer sequence of block layers, which corresponds to the 2H modification, is locally formed adjacent to the stacking fault. These may indicate that the solid-solubility range of the La_5Ni_{19} phase in the La–Ni binary system is very much limited (if present) and that the energy difference among different modifications of La_5Ni_{19}, in particular that between the stable 3R and metastable 2H modifications, is very small.

In La_2Ni_7, stacking faults of the inter-block-layer type, which keeps the number of unit layers in block layers constant (one unit layer of the $LaNi_2$ (Laves)-type and two unit layers of the $LaNi_5$-type), are also observed. However, basal stacking faults of the inter-block-layer type are found to be of the minority in La_2Ni_7 and the majority of stacking faults are of the intra-block-layer type, which is shown in Fig. 4(b). In a particular case of Fig. 4(b), the number of unit layers in block layers are changed from three to six at positions indicated by arrows. We observed changes in the number of unit layers in block layers from three to two or four in other cases. These may indicate that the solid-solubility range of the La_2Ni_7 phase in the La–Ni binary system is wider than that of the La_5Ni_{19} phase and that the stability of the 2H modification of La_2Ni_7 over other possible modifications is high, unlike in the case of the 3R modification of La_5Ni_{19}. The high stability of the 2H modification of La_2Ni_7 over other modifications is consistent with the phase diagram assessment by Buschow and van Goot [12] but not with that by Zhang et al. [8] who inferred the occurrence of the 2H(α)–3R(β) transformation at 976°C from the differential thermal analysis.

3.3. The stability of intermetallic phases in the La–Ni system

Based on the present observations, we revised the accepted phase diagram of the La–Ni binary system near the $LaNi_5$ phase [8,9] (Fig. 5(a)), as shown in Fig. 5(b). The main new aspects in the revised diagram are (i) the presence of the La_5Ni_{19} phase at high temperatures around 1000°C and (ii) the absence of the 2H(α)–3R(β) transformation of the La_2Ni_7 phase at 976°C. The La_5Ni_{19} phase is not stable at low temperatures and decomposes into La_2Ni_7 and $LaNi_5$ phases. The decomposition occurs below a temperature between 900 and 1000°C. We did not observe any evidence for the occurrence of the 3R modification for the La_2Ni_7 phase and thus we believe that the La_2Ni_7 phase of the 2H modification is stable up to its melting temperature. Thus, it seems more natural to ascribe the α–β transformation temperature of the La_2Ni_7 phase [8] to the peritectoid temperature of the phase. Our revised version of the phase diagram is consistent with the prediction by Khan [10].

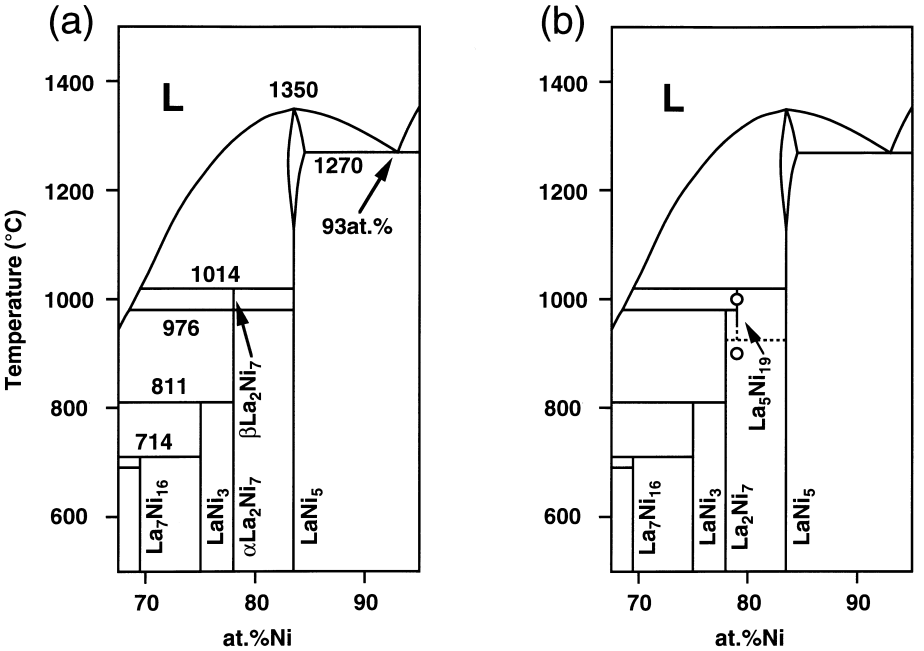

Fig. 5. Partial phase diagrams of the La–Ni binary system near the $LaNi_5$ phase; (a) from [8] and (b) deduced from the present study.

4. Conclusions

1. The intermetallic phase, La_5Ni_{19} is found for the first time to exist as an equilibrium phase between La_2Ni_7 and $LaNi_5$ in the La–Ni binary system. This phase is stable at high temperatures around 1000°C and decomposes into La_2Ni_7 and $LaNi_5$ phases at low temperatures. The crystal structure of La_5Ni_{19} is of the Ce_5Co_{19}-type (3R modification) in which three block layers stack along the c-axis with each block layer consisting of one unit layer of the $LaNi_2$ (Laves)-type and three unit layers of the $LaNi_5$-type.
2. Numerous stacking faults are observed on basal planes in La_5Ni_{19}. Most of them are of the inter-block-layer type in which faulting in the stacking sequence of block layers occurs, keeping the number of unit layers in block layers constant.
3. The density of basal stacking faults is considerably smaller in La_2Ni_7 than in La_5Ni_{19}. Although some stacking faults of the inter-block-layer type are also observed, the majority of faults in La_2Ni_7 are of the intra-block-layer type in which faulting occurs in the number of unit layers in block layers.

Acknowledgements

This work was supported by Grant-in Aid for Scientific Research on Priority Areas (A) of ‘‘New Protium Function’’ from the Ministry of Education, Science, Sports and Culture, Japan and in part by Grant-in-Aid for Scientific Research (No. 08555162) from the Ministry of Education, Science, Sports and Culture, Japan. One of the authors (T.Y.) greatly appreciates the support from Research Fellowship of the Japan Society for the Promotion of Science for Young Scientists.

References

[1] J.H.N. van Vucht, F.A. Kuijpers, H.C.A.M. Bruning, Philips Res. Reports 25 (1970) 133.
[2] J.J.G. Willems, K.H.J. Buschow, J. Less-Comm. Met. 129 (1987) 13.
[3] P.H.L. Notten, R.E.F. Einerhand, Adv. Mater. 3 (1991) 343.
[4] E.H. Kisi, C.E. Buckley, E.M. Gray, J. Alloys Comp. 185 (1992) 369.
[5] K.H.J. Buschow, H.H. van Mal, J. Less-Comm. Met. 29 (1972) 203.
[6] R. Vogel, Z. Metallkd. 38 (1947) 97.
[7] A.V. Virkar, A. Raman, J. Less-Comm. Met. 18 (1969) 59.
[8] D.-Y. Zhang, J.-K. Tang, K.A. Gschneidner Jr., J. Less-Comm. Met. 169 (1991) 45.
[9] Binary Alloy Phase Diagram Updating Service, in: H. Okamoto (Ed.), ASM International, Materials Park, Ohio, USA.
[10] Y. Khan, Z. Metallkd. 65 (1974) 489.
[11] L.S. Ramsdell, Amer. Mineralogist 32 (1947) 64.
[12] K.H.J. Buschow, A.S. van der Goot, J. Less-Comm. Met. 22 (1970) 419.